The magnetic field of an isolated neutron star from X-ray cyclotron absorption lines

G. F. Bignami*†, P. A. Caraveo‡, A. De Luca‡§ & S. Mereghetti‡

** Centre d'Etude Spatiale des Rayonnements, CNRS-UPS, 9 Avenue du Colonel Roche, 31028 Toulouse Cedex 4, France*
† Università degli Studi di Pavia, Dipartimento Fisica Nucleare e Teorica, Via Bassi 6, 27100 Pavia, Italy
‡ Istituto di Astrofisica Spaziale e Fisica Cosmica, Sezione di Milano "G. Occhialini", Via Bassini 15, 20133 Milano, Italy
§ Università di Milano Bicocca, Dipartimento Fisica, Piazza della Scienza 3, 20126 Milano, Italy

Isolated neutron stars are highly magnetized, fast-rotating objects that form as an end point of stellar evolution. They are directly observable in X-ray emission, because of their high surface temperatures. Features in their X-ray spectra could in principle reveal the presence of atmospheres[1], or be used to estimate the strength of their magnetic fields through the cyclotron process[2], as is done for X-ray binaries[3,4]. Almost all isolated neutron star spectra observed so far appear as featureless thermal continua[5,6]. The only exception is 1E1207.4–5209 (refs 7–9), where two deep absorption features have been detected[10,11], but with insufficient definition to permit unambiguous interpretation. Here we report a long X-ray observation of the same object in which the star's spectrum shows three distinct features, regularly spaced at 0.7, 1.4 and 2.1 keV, plus a fourth feature of lower significance, at 2.8 keV. These features vary in phase with the star's rotation. The logical interpretation is that they are features from resonant cyclotron absorption, which allows us to calculate a magnetic field strength of 8×10^{10} G, assuming the absorption arises from electrons.

In August 2002, the XMM-Newton spacecraft devoted two of its orbits to 1E1207.4–5209 for a total observing time of 257,303 s, the longest observation with the EPIC instrument[12,13] on a galactic source. Selecting photons with energies between 0.2–4 keV, inside a 45″ radius from the source, 208,000 photons were found in the PN CCD[12] and 74,600 and 76,700, respectively, in the metal oxide semiconductor CCDs MOS1 and 2 (ref. 13).

Figure 1 shows the spectra of the source as measured by the PN (Fig. 1a) and the two MOS detectors summed together (Fig. 1b). Both independent spectral distributions show, in addition to the two wide absorption features centred at 0.7 and 1.4 keV (refs 10, 11), a third feature around 2.1 keV. The third feature is seen in the three independent PN and MOS1–MOS2 data sets and was also marginally visible in the shorter XMM-Newton observation of December 2001 (ref. 11). The statistical significance of the third feature can now be gauged by the result of an *F*-test. Its inclusion in the overall spectral fit (see Fig. 1 legend) as a gaussian line in absorption yields an improvement in the quality of the fit which has a chance occurrence probability of about 2×10^{-5} for the PN and about 10^{-3} for each of the MOS. A fourth dip at about 2.8 keV is also seen in the PN data and its chance occurrence probability is estimated to be about 5×10^{-2}.

We are aware of the existence of edges of instrumental origin due to Au M (2.209 keV) and Si K (1.839 keV) in the general region of our feature at 2.1 keV. In the spectra of very bright sources, such edges can produce small calibration leftovers (see ref. 14 for example), seen at most at a level of 5%, fully compatible with the EPIC calibration accuracy[15], with an equivalent width of <10 eV (S. Molendi, personal communication). The ~2.1-keV feature present in our spectra is much stronger (with an equivalent width about 15 times higher and deviations from the continuum model at the level of ~25% as opposed to <5%). Moreover, the full-width at half-maximum (FWHM) of our feature is 370 eV, as opposed to the value of 90 eV measured for the calibration leftovers. These characteristics give us confidence about the reality and the non-instrumental nature of our third feature.

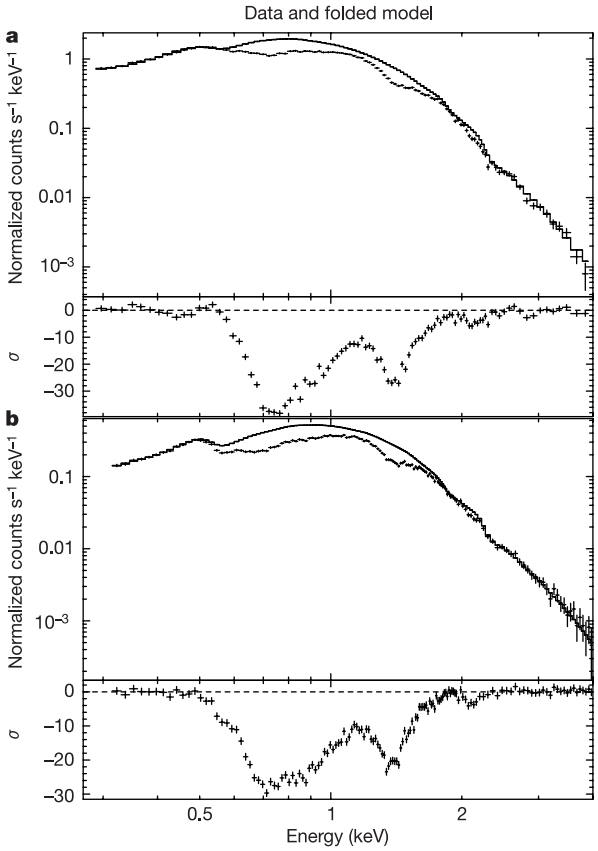

Figure 1 Spectra collected by the PN (**a**) and MOS (**b**) cameras on the EPIC instrument during the observation of 4–6 August 2002. The two MOS cameras were operated in 'full frame' mode[13], and the PN camera was in 'small window' mode for accurate timing of source photons (6-ms resolution[12]). All cameras used the thin filter[13]. The data were processed with the XMM-Newton Science Analysis Software, version 5.3.3. After removing time intervals with high particle background and correcting for dead time, we obtain a net exposure of 138.4 ks for the PN camera and 193.6 and 194.7 ks for the MOS1 and MOS2 cameras, respectively. Our count rates are slightly larger than those reported[11], owing to our use of the thin filter: 1.486 ± 0.003 counts s^{-1} for the PN, 0.379 ± 0.001 counts s^{-1} (MOS1) and 0.388 ± 0.001 counts s^{-1} (MOS2). Data points and best-fitting continuum spectral models are shown, together with residuals in units of standard deviations σ from the best-fitting continuum. The best spectral model ($\chi^2 = 1.25$, 111 degrees of freedom, d.o.f.) describes the continuum as the sum of two blackbody curves with $kT = 0.211 \pm 0.001$ keV, for an emitting radius $R = 2.95 \pm 0.05$ km (assuming a distance $d = 2.2$ kpc; ref. 26), and 0.40 ± 0.02 keV ($R = 250 \pm 50$ m). The line of sight column density, N_H is $(1.0 \pm 0.1) \times 10^{21}$ cm^{-2}, to be compared with 1.6×10^{21} cm^{-2} estimated from radio observations of the associated supernova remnant G296.5 + 10.0 (ref. 26). Any other model for the continuum fails to give such a good fit to the data: we tried a composite (blackbody + power-law) model ($\chi^2 = 1.9$, 111 d.o.f.) and a hydrogen atmosphere model[19] ($\chi^2 = 1.7$, 113 d.o.f.). The central energies of the three absorption features are 0.72 ± 0.02 keV, 1.37 ± 0.02 keV and 2.11 ± 0.03 keV. The possible fourth feature in the PN spectrum is at 2.85 ± 0.06 keV. The optical depths τ for the two main features are similar ($\tau_1 = 0.54 \pm 0.02$; $\tau_2 = 0.52 \pm 0.02$); however, the integrated number of scattered photons is more than four times higher for the feature at 0.7 keV. The third feature is less intense. All errors in the spectral parameters are at the 90% confidence level.

The three absorption features shown in Fig. 1 are wider than the CCD energy resolution and their intensities are definitely different. No significant substructure was detected in any of them. The shapes of the two main features cannot be described by any single gaussian profile. Detailed analytical or numerical fits to the feature shapes are beyond the scope of this work, but we note that at least two gaussian profiles, always larger than the instrument resolution, are needed to describe each of the features at 0.7 and 1.4 keV (see also Fig. 1 legend). In any case, Doppler broadening by thermal electron motion in the $kT \approx 0.2$ keV environment is smaller than the CCD energy resolution. Unfortunately, the higher spectral resolution of the reflection grating spectrometer (RGS)[16] cannot provide any additional clue on this source because its limited sensitivity requires a drastic rebinning of the dispersed data. The resulting spectrum is coarser than those shown in Fig. 1.

After the first EPIC observation, variations of the lines as a function of the pulsar phase were reported[11]. To investigate such an effect in our longer data set, we first had to search for the best source period. This was done following the steps outlined in ref. 11 and yielded a pulsar period $P = 0.42413076 \pm 0.00000002$ s. The light curve for the total energy range (0.2–4 keV), shown in Fig. 2, is characterized by a nearly sinusoidal modulation with a pulsed fraction of about 7%. In it, four phase intervals can easily be identified (see Fig. 2).

Figure 3 shows the four colour-coded spectra corresponding to the four phase intervals. The bulk of the phase dependence of the spectra is seen to be due to the absorption lines variation, while the continua, as seen in the spectral regions not affected by the lines, remain reasonably constant. Indeed, we could go as far as saying that the X-ray source pulsation is largely due to the phase variation of the lines with the neutron star rotation. To our knowledge, this is the first time that such a phenomenon has been observed for a rotating compact object. The inset to Fig. 3 allows for a direct appreciation of the absorption feature phase variation, as seen through the spectral residuals.

To summarize, the soft X-ray spectrum of 1E1207.4 − 5209 is characterized by three absorption features with integrally spaced energies (0.7, 1.4 and 2.1 keV; there may even be a fourth one at ~2.8 keV), and which are varying in phase with the neutron star rotation, possibly accounting for the bulk of the X-ray pulsation. They also have, in our deep XMM-Newton observation, an extent, or depth, which appears to be globally decreasing with energy (see Fig. 1), although this effect appears to be phase-dependent.

X-ray spectral features from an isolated neutron star (INS) can be due to atomic transition lines, photoabsorption edges or cyclotron lines. The atmosphere of an INS is a very difficult environment for physics, owing to the necessity of working with an *a priori* unknown nuclear species composition and level of ionization, in a Landau regime of high magnetic field. We refer to extensive work[17,18] on possible transition lines or photoabsorption edges. Their final preference for explaining the Chandra features in 1E1207.4 − 5209 with He-like mid-Z (O or Ne) absorption lines, although certainly self-consistent, seems no longer justified by the present XMM-Newton data.

Atmospheric absorption models[1,19] also meet with the strong difficulty of the lack of similar features in any of the several INSs for which good Chandra/XMM-Newton spectra are now available. Data for such diverse INSs as Vela, pulsars PSR B0656 + 14 and PSR B1055 − 52, the millisecond pulsar PSR J0437 − 4715 and the two 'dim' INSs RX J1856.5 − 3754 and RX J0720.4 − 3125 (see recent reviews[5,6]) were explored and none shows absorption or emission features. These objects cover a vast range in age (from 10^4 yr to 'eternity' in the case of the millisecond pulsar), in magnetic fields B, in possible interstellar accretion rate, and so on. It is difficult to imagine none of these INSs showing a phenomenology similar to 1E1207.4 − 5209, if the features of the latter were due to atmospheric absorption.

Occam's razor, in the end, leads us to conclude that cyclotron resonance scattering explains the features presented above: three lines, correctly spaced by integral factors (within the uncertainties on their measured centroids) and with a phase variation naturally following the pulsar B-field rotation, as observed for the much brighter accreting neutron stars in binary systems, see refs 20, 21 for example.

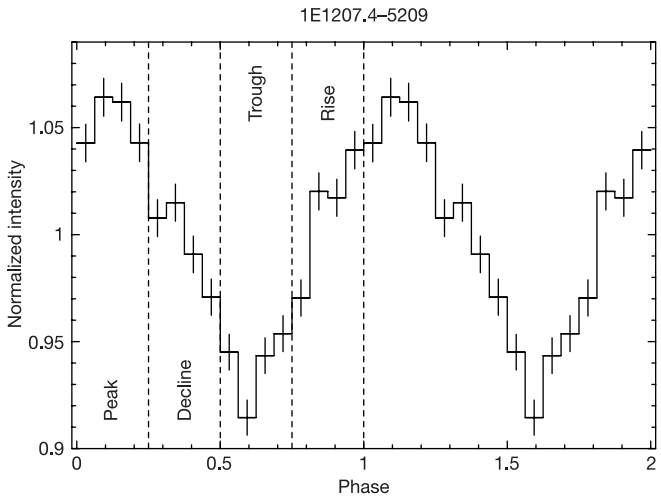

Figure 2 Total light curve relative to 208,000 photons collected by the PN camera folded at the best period of $P = 0.42413076$ s. When compared to the Chandra measurement of January 2000 (refs 9, 30), this yields a refined estimate of the pulsar spindown of $\dot{P} = (1.4 \pm 0.3) \times 10^{-14}$ s s^{-1}. The four equal phase intervals used to assess the spectral variation (namely, 'peak', 'decline', 'trough' and 'rise') are also shown.

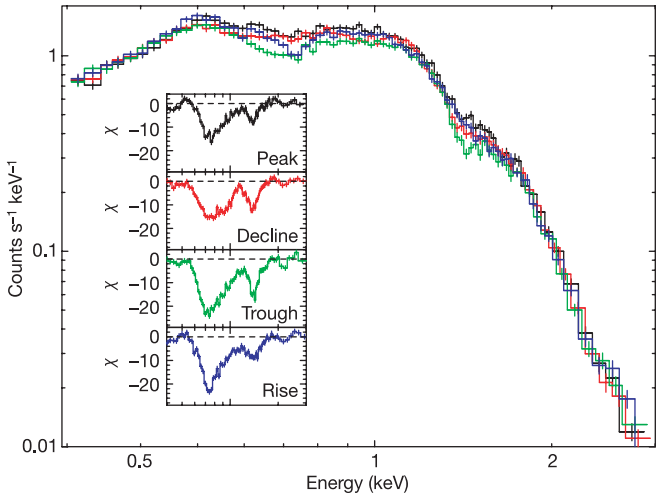

Figure 3 Comparison of the four PN spectra for phase intervals as defined in Fig. 2. Note that absolute (counts s^{-1} keV^{-1}) spectra are plotted. Colours indicate spectral variation: black, peak; red, decline; green, trough; blue, rise. The peak of the total light curve corresponds to the phase interval where the absorption lines are at their minimum (black data points) while the light-curve trough happens when the absorption lines are more important (green data points). Inset, the four panels show the residuals of the phase-dependent spectra from the two-blackbody fit used in Fig. 1a. Phase variations in both shape and intensity for all features are apparent. The comparison of phase-dependent residuals with Fig. 3 of ref. 11 shows the improvement achieved with the present long observation.

Note that small deviations from the 1:2:3 ratio of the line centroids can also be induced by the complex geometrical and physical environment related to harmonic generation[22]. Our best-fitting temperature for the source continuum emission ($\sim$0.21 keV) is nicely consistent with the equilibrium Compton temperature due to resonant scattering, computed[2] to be 0.27 of the energy of the first harmonic, or about 0.19 keV.

Following ref. 23, we note that in cyclotron scattering above the surface of an INS, the cross-section (and the relative strength of the harmonic lines) depends on the angle between the observer and the magnetic field. This provides a natural explanation for the phase variation of the feature depths. There are also compelling physical reasons[23,24] why all line widths should vary in phase, with maximum broadening appearing when the observer's line of sight and the pulsar B field are aligned. Of course, such asymmetric and varying line profiles render problematic any precise evaluation of each line's central energy as well as their harmonic spacings. Thus, *a fortiori*, considerations on line shapes and their centroid energies based on the phase-averaged spectra of Fig. 1 have little physical meaning. Rather, any physical interpretative work on 1E1207.4 − 5209 should be driven by phase-resolved spectroscopy.

If the $\sim$0.7-keV line is the fundamental electron cyclotron frequency, then B averaged over the star's disk is around 6×10^{10} $(1 + z)$, or 8×10^{10} G, assuming a 'standard' 20% gravitational redshift, z. For protons, the field should be higher by a factor equal to the proton-to-electron mass ratio, yielding $B = 1.6 \times 10^{14}$ G, that is, a magnetar-type magnetic field[25]. Neither of these values agrees with the B field inferred from the 1E1207.4 − 5209 timing parameters, which give $(2–3) \times 10^{12}$ G under the rotating dipole hypothesis. This hypothesis, however, is not problem-free for our object because the current period derivative, $\dot{P} = (1.4 \pm 0.3) \times 10^{-14}$ s s^{-1} implies a pulsar age of about 4.8×10^5 yr, which is totally incompatible with that of the supernova remnant associated with it, no more than about 10^4 yr old[26]. Although the reported tentative radio detection[27] may help to monitor the pulsar timing parameters better, it seems unlikely that improved timing could solve the age inconsistency problem. More drastic assumptions, such as low spin frequency at birth, should possibly be considered.

To reconcile the pulsar period derivative and the B value inferred in the case of electron cyclotron emission close to the neutron star surface, one should invoke additional pulsar braking mechanisms, such as the debris disk configuration proposed[28]. Of course, electron cyclotron scattering at a distance $R \approx 3–4$ stellar radii (that is, 20–30 km above the neutron star surface) would fit all the observations.

Alternatively, the cyclotron features could be due to protons. This would require an improbable surface magnetic field about 100 times stronger than that deduced from the spindown. Although a single proton cyclotron feature could be present in the optical spectrum of Geminga[29], the B-field requirements for 1E1207.4 − 5209 seem too large to support the proton cyclotron explanation for the observed X-ray features.

On the whole, electron resonance scattering in an abnormally low magnetic field seems to explain the current XMM-Newton observations best. The cyclotron nature of the features, as opposed to the atmospheric one, would also naturally explain the uniqueness of the 1E1207.4 − 5209 spectrum in the INS context, because the powerful combination of throughput and energy resolution of XMM-Newton/EPIC is only effective for less than a decade in photon energy. Most INSs, with a more normal B field, may have electron cyclotron features in the 10–20 keV range, that is, where such features were observed for the much brighter accreting objects. □

Received 3 February; accepted 6 May 2003; doi:10.1038/nature01703.

1. Zavlin, V. E. & Pavlov, G. G. *Modeling Neutron Star Atmospheres* (eds Becker, W., Lesch, H. & Trümper, J.) 263–272 (MPE Report 278, Max Plank Institut für Extraterrestrische Physik, Garching bei, München, 2002).
2. Lamb, D. Q., Wang, J. C. L. & Wasserman, I. M. Energetics and dynamics of resonant and nonresonant scattering in strong magnetic fields. *Astrophys. J.* **363,** 670–693 (1990).
3. Trümper, J. *et al.* Evidence for strong cyclotron line emission in the hard X-ray spectrum of Hercules X-1. *Astrophys. J.* **219,** L105–L110 (1978).
4. Weathon, Wm. A. *et al.* An absorption feature in the spectrum of the pulsed hard X-ray flux from 4U0115 + 63. *Nature* **282,** 240–243 (1979).
5. Pavlov, G. G., Zavlin, V. E. & Sanwal, D. *Thermal Radiation from Neutron Stars: Chandra Results* (eds Becker, W., Lesch, H. & Trümper, J.) 273–289 (MPE Report 278, Max Plank Institut für Extraterrestrische Physik, Garching bei, München, 2002).
6. Becker, W. & Aschenbach, B. in *X-ray Observations of Neutron Stars and Pulsars: First Results from XMM-Newton* (eds Becker, W., Lesch, H. & Trümper, J.) 64–86 (MPE Report 278 Max Plank Institut für Extraterrestrische Physik, Garching bei, München, 2002).
7. Bignami, G. F., Caraveo, P. A. & Mereghetti, S. On the optical counterpart of 1E1207.4−5209, the central X-ray source of a ring-shaped supernova remnant. *Astrophys. J.* **389,** L67–L69 (1992).
8. Caraveo, P. A., Bignami, G. F. & Trümper, J. Radio-silent isolated neutron stars as a new astronomical reality. *Astron. Astrophys. Rev.* **7,** 209–216 (1996).
9. Zavlin, V. E., Pavlov, G. G., Sanwal, D. & Trümper, J. Discovery of 424 millisecond pulsations from the radio-quiet neutron star in the supernova remnant PKS1209 − 51/52. *Astrophys. J.* **540,** L25–L28 (2000).
10. Sanwal, D., Pavlov, G. G., Zavlin, V. E. & Teter, M. A. Discovery of absorption features in the X-ray spectrum of an isolated neutron star. *Astrophys. J.* **574,** L61–L64 (2002).
11. Mereghetti, S. *et al.* Pulse phase variations of the X-ray spectral features in the radio-quiet neutron star 1E1207 − 5209. *Astrophys. J.* **581,** 1280–1285 (2002).
12. Strüder, L. *et al.* The European photon imaging camera on XMM-Newton: The pn-CCD camera. *Astron. Astrophys.* **365,** L18–L26 (2001).
13. Turner, M. *et al.* The European photon imaging camera on XMM-Newton: The MOS cameras. *Astron. Astrophys.* **365,** L27–L35 (2001).
14. Miller, J. M. *et al.* XMM-Newton spectroscopy of the accretion-driven millisecond X-ray pulsar XTE J1751 − 305 in outburst. *Astrophys. J.* **583,** L99–L102 (2003).
15. Kirsch, M. (on behalf of the EPIC collaboration) *EPIC Calibration Issues in Progress* Document XMM-SOC-CAL-TN-0018 (EPIC Status of Calibration and Data Analysis), XMM-Newton Science Operation Centre, Villafranca del Castillo, 2002); ⟨http://xmm.vilspa.esa.es/docs/documents/CAL-TN-0018-2-0.pdf⟩.
16. Den Herder, J. W. *et al.* The reflection grating spectrometer on board XMM-Newton. *Astron. Astrophys.* **365,** L7–L17 (2001).
17. Mori, K. *et al.* X-ray spectroscopy of the isolated neutron star 1E1207.4 − 5209: Atmospheric composition and equation of state. *Astrophys. J.* (submitted); preprint at ⟨http://arXiv.org/astro-ph/0301161⟩ (2003).
18. Hailey, C. J. & Mori, K. Evidence of a mid-atomic number atmosphere in the neutron star 1E1207.4 − 5209. *Astrophys. J.* **578,** L133–L136 (2002).
19. Zavlin, V. E., Pavlov, G. G. & Shibanov, Yu. Model neutron star atmospheres with low magnetic fields. I. Atmospheres in radiative equilibrium. *Astron. Astrophys.* **315,** 141–152 (1996).
20. Voges, W. *et al.* Cyclotron lines in the hard X-ray spectrum of Hercules X-1. *Astrophys. J.* **263,** 803–813 (1982).
21. Nagase, F. *et al.* Cyclotron line features in the spectrum of the transient X-ray pulsar X0115 + 634. *Astrophys. J.* **375,** L49–L52 (1991).
22. Isenberg, M., Lamb, D. Q. & Wang, J. C. L. Effects of the geometry of the line-forming region on the properties of cyclotron resonant scattering lines. *Astrophys. J.* **505,** 688–714 (1998).
23. Freeman, P. E. *et al.* Resonant cyclotron radiation transfer model fits to spectra from gamma-ray burst GRB 870303. *Astrophys. J.* **524,** 772–792 (1999).
24. Meszaros, P. & Nagel, W. X-ray pulsar models. I—Angle-dependent cyclotron line formation and comptonization. *Astrophys. J.* **298,** 147–160 (1985).
25. Zane, S. *et al.* Proton cyclotron features in thermal spectra of ultramagnetized neutron stars. *Astrophys. J.* **560,** 384–389 (2001).
26. Giacani, E. B. *et al.* The interstellar matter in the direction of the supernova remnant G296.5 + 10.0 and the central X-ray source 1E1207.4 − 5209. *Astron. J.* **119,** 281–291 (2000).
27. Camilo, F. Deep searches for young pulsars. *ASP Conf. Ser.* (eds Bailes, M., Nice, D. J. & Thorsett, S.) (Astronomical Society of the Pacific, San Francisco, in the press); preprint at ⟨http://arXiv.org/astro-ph/0210620⟩.
28. Xu, R. X., Wang, H. G. & Qiao, G. J. A note on the discovery of absorption features in 1E1207.4 − 5209. *Chin. Phys. Lett.* **20,** 314 (2003); preprint at ⟨http://arXiv.org/astro-ph/0207079⟩.
29. Bignami, G. F. *et al.* Multiwavelength data suggest a cyclotron feature on the hot thermal continuum of Geminga. *Astrophys. J.* **456,** L111–L114 (1996).
30. Pavlov, G. G., Zavlin, V. E., Sanwal, D. & Trümper, J. 1E 1207.4 − 5209: The puzzling pulsar at the center of the supernova remnant PKS 1209 − 51/52. *Astrophys. J.* **569,** L95–L98 (2002).

Acknowledgements We thank F. Jansen and all the XMM-Newton team in Vilspa for approving and carrying out this target of opportunity observation at very short notice. We also thank W. Becker and M. Turner for helping us to optimize EPIC settings. G.F.B. acknowledges discussions with D. Lamb, G. Ricker and J. Doty about the cyclotron line interpretation of the spectral features of this object. The XMM-Newton data analysis is supported by the Italian Space Agency (ASI). A.D.L. acknowledges an ASI fellowship.

Competing interests statement The authors declare that they have no competing financial interests.

Correspondence and requests for materials should be addressed to G.F.B. (bignami@cesr.fr).